JOURNAL OF GUIDANCE, CONTROL, AND DYNAMICS
Vol. 30, No. 5, September–October 2007

Parameter-Free Second-Order Numerical Scheme for Constrained Multibody Dynamic Systems

Samuel W. J. Welch*
University of Colorado at Denver and Health Sciences Center, Denver, Colorado 80217-3364
Min Hong†
Soonchunhyang University, Asan 336-745, Republic of Korea
and
John A. Trapp‡ and Min-Hyung Choi§
University of Colorado at Denver and Health Sciences Center, Denver, Colorado 80217-3364

DOI: 10.2514/1.28708

This paper describes a second-order numerical scheme for constrained multibody dynamics that is simple to implement and does not require the selection of parameters for constraint satisfaction. The method is a predictor–corrector type of method, and both the predictor and the corrector steps require solution of a symmetric positive-definite linear system with no iteration of nonlinear equations. The basic philosophy of the method is to satisfy the constraint equations to the same order as the discretization of the ordinary differential equations.

Nomenclature

C = coefficient in error expansion
E = total energy
E_o = initial total energy
e = vector of Euler parameters
F = applied force
f = state derivative vector
G = matrix defining relationship between Euler parameters and angular velocities
g = gravity
h = midpoint superscript
J = inertia matrix or value
M = mass matrix
n = local truncation error exponent
O = order identifier
p = predictor superscript
Q = generalized force
q = generalized coordinate
r = center of mass coordinate
T = applied torque
t = time
x, y = center of gravity coordinates used in the planar example
a, β = Baumgarte parameters
Δt = time step
ε_E = relative change of total energy
θ = orientation angle for planar systems
λ = vector of Lagrange multipliers
Φ = vector of holonomic constraints
$\bar{\Phi}$ = mean value of magnitude of constraints over simulation duration
Φ_q = constraint Jacobian with regard to generalized coordinates
Φ_r = constraint Jacobian with regard to center of mass coordinates
Φ_π = constraint Jacobian with regard to orientation coordinates
ϕ = orientation angle used in planar simulation example
Ψ = normalization constraint for Euler parameters
ω = angular velocity vector
$\tilde{\omega}$ = antisymmetric matrix associated with the angular velocity

I. Introduction

THE simulation of multibody dynamic systems has become an important tool in the design and understanding of complex mechanical systems. The equations describing multibody dynamic systems may be written as a system of differential algebraic equations (DAEs), and there is a growing body of literature directed toward the solution of DAEs. Early techniques for solution of DAEs differentiated the algebraic constraints, thereby reducing DAEs to a system of ordinary differential equations (ODEs). The resulting solutions did not satisfy the algebraic constraint equations, motivating the stabilization method of Baumgarte [1]. Using two arbitrary parameters, Baumgarte added stabilizing terms to the twice-differentiated constraint equations, thus mimicking a classical second-order system, with the response settling to a null value. It is a testament to the value of Baumgarte's idea that after more than three decades, his method is still widely used. Baumgarte's method is easily incorporated into schemes using standard techniques for integrating ODEs. Recent examples are Wu et al. [2], who used Baumgarte's stabilization technique along with a modified Adams–Moulton predictor–corrector method, and Lin and Huang [3], who used Baumgarte's stabilization in their implementation of a predictor–corrector method and in their implementation of a Runge–Kutta method [4].

Despite the wide acceptance of Baumgarte's stabilization, the method is often found wanting, due to the difficulty in establishing optimal parameters. Improper selection of the parameters may result in artificially stiff systems or inadequate satisfaction of the constraints. These shortcomings are often cited by authors as

Received 4 November 2006; revision received 1 April 2007; accepted for publication 2 April 2007.

*Associate Professor, Mechanical Engineering, P.O. Box 173364, Campus Box 112.
†Lecturer, Division of Computer Science and Engineering, 646 Eupnae-Ri Shinchang-Myeon Asan-Si, Chungcheongnam-Do.
‡Professor, Mechanical Engineering, P.O. Box 173364, Campus Box 112.
§Associate Professor, Computer Science and Engineering, P.O. Box 173364, Campus Box 109.

precipitating factors in the search for improved methods. Improved stabilization methods include the methods of Park and Chiou [5] and Ascher et al. [6]. In both cases, a single parameter, ostensibly easier to determine than the Baumgarte parameters, is required. Parameter-free, albeit more complicated, techniques are given by Negrut et al. [7], who describe an implicit technique based on coordinate partitioning that is particularly suited for solution of stiff systems, and Aghili and Piedboeuf [8], who describe a technique based upon a projection operator. Brenan et al. [9] discuss at length the popular backward differentiation formula methods, which are implicit methods requiring iteration to complete a time step. Comprehensive surveys of existing techniques for handling the DAEs associated with constrained multibody dynamics are provided in [6] and in [7]. In this paper, we will present an approach that is parameter-free and is based upon the idea of expanding the algebraic constraint at the new time level in a Taylor series to the same order as the order of the numerical method used to integrate the ODE system. An implicit first-order version of this approach has been applied to planar dynamic simulations [10] and mass-spring networks [11], and a semi-implicit first-order version of this method has been applied to multibody dynamics [11,12]. In this paper, we will demonstrate the approach by developing a second-order method for holonomically constrained systems of rigid bodies. Extension to systems with nonholonomic constraints is straightforward, and a first-order version of this is given in [12]. The advantages to this approach are simplicity and the fact that the associated methods are parameter-free. The disadvantage to the approach is that unlike the methods mentioned earlier, it is not simple to obtain a modified ODE that can be cast into state-space form and solved to arbitrary order using standard ODE packages or methods.

II. Basic Equations

We will consider a set of dynamic equations written for a system of rigid bodies using the Cartesian coordinates of the mass centers for translational variables and Euler parameters for the rotational variables. Let Φ be the vector of scleronomic constraints written using center of mass coordinates r and the Euler parameters e. Let λ be a vector containing the Lagrange multipliers and let Φ_r and Φ_π be the constraint Jacobian matrices associated with r and Φ_π the orientation; that is, the differentiated constraint has the form

$$\Phi_r \dot{r} + \Phi_\pi \omega = 0 \tag{1}$$

Note that Φ_π is not truly a Jacobian but may be seen as the coefficient of a virtual rotation in a differential expansion of the constraint equation [13]. The equations of motion for this constrained system with mass matrix M, applied force F, and inertia matrix J are written as

$$M\ddot{r} + \Phi_r^T \lambda = F \tag{2}$$

$$J\dot{\omega} + \Phi_\pi^T \lambda = T - \tilde{\omega} J \omega \tag{3}$$

$$\Phi(r, e) = 0 \tag{4}$$

where $\tilde{\omega}$ is the skew-symmetric matrix associated with the angular velocity:

$$\tilde{\omega} = \begin{bmatrix} 0 & -\omega_3 & \omega_2 \\ \omega_3 & 0 & -\omega_1 \\ -\omega_2 & \omega_1 & 0 \end{bmatrix} \tag{5}$$

Alternatively, the equations of motion may be written using generalized coordinates with generalized forces:

$$M\ddot{q} + \Phi_q^T \lambda = Q \tag{6}$$

$$\Phi(q) = 0 \tag{7}$$

where $q = [r\ e]^T$ for three-dimensional systems and $q = [r\ \theta]^T$ for two-dimensional systems. Note that M in Eq. (6) is not the same as M in Eq. (2). Should the constraint be of the form $\Phi(r, e, t) = 0$ (i.e., rheonomic), the additional terms required in our numerical treatment are easily included (see, for example, Hong et al. [12]). For three-dimensional problems, the kinematic relationship between the Euler parameters and the angular velocity may be written as [13]

$$\dot{e} = H(e)\omega \tag{8}$$

where

$$H(e) = \frac{1}{2}\begin{bmatrix} -e_1 & e_0 & e_3 & -e_2 \\ -e_2 & -e_3 & e_0 & e_1 \\ -e_3 & e_2 & -e_1 & e_0 \end{bmatrix} \tag{9}$$

This may be written as

$$\dot{e} = G(\omega)e \tag{10}$$

where

$$G(\omega) = \frac{1}{2}\begin{bmatrix} 0 & -\omega^T \\ \omega & -\tilde{\omega} \end{bmatrix} \tag{11}$$

We note also that the Euler parameters must satisfy the normalization constraint Ψ:

$$\Psi(e) = e^T e - 1 = 0 \tag{12}$$

This constraint is incorporated into the kinematic relationship [Eq. (11)], but truncation and round-off errors cause the Euler parameters to drift from their normalized state; thus, the normalization constraint will be included in the numerical treatment of the equations of motion. It is possible to include the normalization constraint with the other holonomic constraints (Haug [13]), but we will not do so here.

III. Algebraic Constraint Enforcement

The second-order method developed here will be a predictor–corrector type of algorithm including algebraic constraint enforcement. The basic philosophy of the algebraic constraint enforcement technique is to expand the algebraic constraint function at the new time level in a Taylor series with the base point at the previous time level. The Taylor series expansion will be to the same order as the discrete equations forming the numerical approximation to the ordinary differential equations comprising the dynamic system. In the development that follows, the applied forces F, the generalized forces Q, and the applied moments T are considered constant. Extension of the method to nonconstant F, Q, and T is straightforward.

The predictor step is a first-order step, thus we discretize the system of differential equations to first order (globally). For example, Eq. (2) is discretized as

$$\dot{r}(t + \Delta t) = \dot{r}_n + \Delta t M^{-1} F - \Delta t M^{-1} \Phi_r^T \lambda^p + \mathcal{O}(\Delta t^2) \tag{13}$$

and this may be written using the predicted variable $\dot{r}^p_{n+1}$ as

$$\dot{r}^{\,p}_{n+1} = \dot{r}_n + \Delta t M^{-1} F - \Delta t M^{-1} \Phi_r^T \lambda^p \tag{14}$$

In a similar manner, the other differential equations in the system are discretized to the same order as

$$r^p_{n+1} = r_n + \Delta t \dot{r}^p_{n+1} \tag{15}$$

$$\omega^p_{n+1} = \omega_n + \Delta t J^{-1} T - \Delta t J^{-1} \tilde{\omega}_n J \omega_n - \Delta t J^{-1} \Phi_\pi^T \lambda^p \tag{16}$$

$$e^p_{n+1} = e_n + \Delta t G\left(\omega^p_{n+1}\right) e^p_{n+1} \tag{17}$$

Here and in the following text, the subscript $n+1$ refers to the new time-level approximation and the subscript n refers to the old time-level approximation. Note that the term $\dot{r}^p_{n+1}$ n the right-hand side of Eq. (15) and the term $G(\omega^p_{n+1})e^p_{n+1}$ on the right-hand side of Eq. (17) are written at new time, because the resulting implicitness comes at little computational cost. In these equations and in all equations that follow, terms without explicit time dependence indicated are evaluated at old time. Note that the explicit treatment of the term $\tilde{\omega}_n J\omega_n$ results in the overall scheme being semi-implicit. We use generalized coordinates (for notational simplicity) to write the appropriate Taylor series expansion of the constraint equations at new time as

$$\Phi(t+\Delta t) = \Phi^n + \Phi_q\{q(t+\Delta t) - q_n\} + \mathcal{O}\Big[q(t+\Delta t) - q_n\Big]^2 = 0 \tag{18}$$

Equation (15) may be used to eliminate the new time coordinates and quantifies the local truncation error as first order (second order locally):

$$\Phi^n + \Phi_q\Big\{\dot{q}^p_{n+1}\Delta t\Big\} + \mathcal{O}(\Delta t)^2 = 0 \tag{19}$$

We note that this equation is a discretization of the ordinary differential equation $\Phi(t) + \Delta t\dot{\Phi}(t) = 0$, which may be viewed as a stabilization of the once-differentiated constraint $[\dot{\Phi}(t) = 0]$ that is known to drift. Returning to the translational and rotational variables, we have

$$\Phi^n + \Big\{\Phi_r\dot{r}^p_{n+1} + \Phi_\pi\omega^p_{n+1}\Big\}\Delta t = 0 \tag{20}$$

Equations (14) and (16) may be used to eliminate $\dot{r}^p_{n+1}$ and ω^p_{n+1}, resulting in the symmetric positive-definite linear system that must be solved for the Lagrange multiplier:

$$\Big[\Phi_r M^{-1}\Phi_r^T + \Phi_\pi J^{-1}\Phi_\pi^T\Big]\lambda^p = \frac{\Phi}{\Delta t^2} + \frac{1}{\Delta t}(\Phi_r\dot{r}_n + \Phi_\pi\omega_n) + \Phi_r M^{-1}F + \Phi_\pi J^{-1}(T - \tilde{\omega}_n J\omega_n) \tag{21}$$

Once this system is solved for the Lagrange multipliers, Eqs. (14–16) are used to update the other variables. In this work, M and J are assumed positive definite and the constraints are independent, thus $[\Phi_r\Phi_\pi]$ has full rank and the linear system $[\Phi_r M^{-1}\Phi_r^T + \Phi_\pi J^{-1}\Phi_\pi^T]$ is positive definite.

The Euler parameters obtained from Eq. (17) are normalized by using the one-step poststabilization method of Greenwood [14] that adjusts the Euler parameters by the increment

$$\Delta e = -\frac{e}{2}\frac{\Psi}{|e|} \tag{22}$$

thus the error in the normalization constraint is eliminated. Note that this correction does not change the direction of e in 4-space [14]. This predictor step is the first-order scheme presented by Hong et al. [12] and has been extended to treat nonholonomic constraints [12].

The corrector step is a second-order centered step using half-time variables. The predicted new time variables are used to calculate required half-time variables as follows (predictor step variables are denoted with a superscript p):

$$r^h = \tfrac{1}{2}\Big\{r^p_{n+1} + r_n\Big\} \tag{23}$$

$$e^h = \tfrac{1}{2}\Big\{e^p_{n+1} + e_n\Big\} \tag{24}$$

$$\omega^h = \tfrac{1}{2}\Big\{\omega^p_{n+1} + \omega_n\Big\} \tag{25}$$

The half-time variables are used to calculate the half-time constraint Jacobian:

$$\Phi^h_r = \Phi_r(r^h, e^h) \tag{26}$$

$$\Phi^h_\pi = \Phi_\pi(r^h, e^h) \tag{27}$$

The half-time (or centered) constraint Jacobians are then used to form the centered finite difference approximation to the ordinary differential equations in the system. For example, the centered discretization of Eq. (2) is

$$\dot{r}(t+\Delta t) = \dot{r}_n - \Delta t M^{-1}\Phi_r^{hT}\lambda + \Delta t M^{-1}F + \mathcal{O}(\Delta t^3) \tag{28}$$

and this may be written using the new time approximation $\dot{r}_{n+1}$ as

$$\dot{r}_{n+1} = \dot{r}_n - \Delta t M^{-1}\Phi_r^{hT}\lambda + \Delta t M^{-1}F \tag{29}$$

In a similar manner, the other differential equations in the system are discretized to the same order as

$$r_{n+1} = r_n + \frac{\Delta t}{2}[\dot{r}_{n+1} + \dot{r}_n] \tag{30}$$

$$\omega_{n+1} = \omega_n - \Delta t J^{-1}\Phi_\pi^{hT}\lambda + \Delta t J^{-1}T - \Delta t J^{-1}\tilde{\omega}^h J\omega^h \tag{31}$$

$$e_{n+1} = e_n + \frac{\Delta t}{2}G\left(\frac{1}{2}[\omega_{n+1} + \omega_n]\right)(e_{n+1} + e_n) \tag{32}$$

As before, the Euler parameters obtained from Eq. (32) are normalized.

The final step in the development of the second-order scheme is to find an appropriate second-order expansion of the algebraic constraint equation. We begin by expanding the constraint equation about the predicted variables (again, generalized coordinates are used for notational simplicity).

$$\Phi(t+\Delta t) = \Phi^p + \Phi^p_q\{q(t+\Delta t) - q^p\} + \mathcal{O}(q(t+\Delta t) - q^p)^2 \tag{33}$$

Because $q(t+\Delta t) - q^p = \mathcal{O}(\Delta t^2)$, the expansion given by Eq. (33) is third order globally. This is one order more than is needed and in what follows, we will write this expression using the half-time Jacobian that appears in Eqs. (29) and (31) with a view toward developing a symmetric positive-definite linear system to be solved for the Lagrange multipliers. If we expand the constraint Jacobian about the half-step we find

$$\Phi^p_q = \Phi^h_q + \Phi^h_{qq}\Big(q^p_{n+1} - q^h\Big) + \mathcal{O}\Big(q^p_{n+1} - q^h\Big)^2 \tag{34}$$

where Φ_{qq} is the derivative of Φ_q with respect to q [13]. Now $q^p_{n+1} - q^h$ may be expressed as

$$q^p_{n+1} - q^h = \tfrac{1}{2}\Big(q^p_{n+1} - q_n\Big) = \tfrac{1}{2}\Delta t\dot{q}^p_{n+1} + \mathcal{O}(\Delta t^2) \tag{35}$$

thus,

$$\Phi^p_q = \Phi^h_q + \mathcal{O}(\Delta t) \tag{36}$$

and we may write the expansion given by Eq. (33) to second order (globally) if we use the half-step Jacobian:

$$\Phi(t+\Delta t) = \Phi^p + \Phi^h_q\{q(t+\Delta t) - q^p\} + \mathcal{O}(\Delta t)^3 \tag{37}$$

This reduction of order of this expansion results in an expansion that is still second order and, as will be shown, the benefit is that we obtain a symmetric positive-definite linear system to be solved for the Lagrange multipliers. Next, we add and subtract the term $\Phi^h_q q(t)$ to Eq. (37), resulting in

$$\Phi(t+\Delta t) = \Phi^p + \Phi^h_q\{q(t+\Delta t) - q(t)\} - \Phi^h_q\{q^p - q(t)\} + \mathcal{O}(\Delta t)^3 \tag{38}$$

The discrete kinematic equations from the predictor [Eq. (15)] and corrector [Eq. (30)] steps are used to eliminate the bracketed terms on the right-hand side, resulting in

$$\Phi(t+\Delta t) = \Phi^p + \Phi^h_q \frac{\Delta t}{2}\{\dot q_{n+1} + \dot q_n\} - \Phi^h_q\{\Delta t \dot q^p\} + \mathcal{O}(\Delta t)^3 \tag{39}$$

Returning to the translational and rotational variables, we rewrite Eq. (39) as

$$\Phi(t+\Delta t) = \Phi^p + \frac{\Delta t}{2}\left\{\Phi^h_r \dot r_{n+1} + \Phi^h_\pi \omega_{n+1}\right\} + \frac{\Delta t}{2}\left\{\Phi^h_r \dot r_n + \Phi^h_\pi \omega_n\right\} - \Delta t\left\{\Phi^h_r \dot r^p_{n+1} + \Phi^h_\pi \omega^p_{n+1}\right\} + \mathcal{O}(\Delta t)^3 \tag{40}$$

The corrector momentum equations may now be used to eliminate $\dot r_{n+1}$ and ω_{n+1} with the result

$$\Phi(t+\Delta t) = \Phi^p - \Delta t\left\{\Phi^h_r \dot r^p_{n+1} + \Phi^h_\pi \omega^p_{n+1}\right\} + \frac{\Delta t}{2}\Phi^h_r\left\{2\dot r_n - \Delta t M^{-1}\Phi^{hT}_r \lambda + \Delta t M^{-1} F\right\} + \frac{\Delta t}{2}\Phi^h_\pi\left\{2\omega_n - \Delta t J^{-1}\Phi^{hT}_\pi \lambda + \Delta t J^{-1} T - \Delta t J^{-1}\tilde\omega^h J\omega^h\right\} + \mathcal{O}(\Delta t)^3 \tag{41}$$

Equation (41) is now set equal to zero; the approximation may be rearranged to express the symmetric positive-definite system that must be solved for the corrected Lagrange multipliers:

$$\left[\Phi^h_r M^{-1}\Phi^{hT}_r + \Phi^h_\pi J^{-1}\Phi^{hT}_\pi\right]\lambda = \frac{2\Phi^p}{\Delta t^2} + \frac{2\Phi^h_r}{\Delta t}\left(\dot r_n - \dot r^p_{n+1}\right) + \frac{2\Phi^h_\pi}{\Delta t}\left(\omega_n - \omega^p_{n+1}\right) + \Phi^h_r M^{-1} F + \Phi^h_\pi J^{-1}(T - \tilde\omega^h J\omega^h) \tag{42}$$

After solution of this system for the Lagrange multipliers, Eqs. (29–32) are used to update the other variables. The complete second-order scheme may be summarized in the following algorithm written for the three-dimensional case:

Predictor step:

$$\begin{aligned}
&\left[\Phi_r M^{-1}\Phi^T_r + \Phi_\pi J^{-1}\Phi^T_\pi\right]\lambda^p = \frac{\Phi}{\Delta t^2} + \frac{1}{\Delta t}(\Phi_r \dot r_n + \Phi_\pi \omega_n) + \Phi_r M^{-1} F + \Phi_\pi J^{-1}(T - \tilde\omega_n J\omega_n)\\
&\dot r^p_{n+1} = \dot r_n + \Delta t M^{-1} F - \Delta t M^{-1}\Phi^T_r \lambda^p\\
&r^p_{n+1} = r_n + \Delta t \dot r^p_{n+1}\\
&\omega^p_{n+1} = \omega_n + \Delta t J^{-1} T - \Delta t J^{-1}\tilde\omega_n J\omega_n - \Delta t J^{-1}\Phi^T_\pi \lambda^p\\
&e^p_{n+1} = e_n + \Delta t G\left(\omega^p_{n+1}\right) e^p_{n+1}\\
&e^{pT}_{n+1} e^p_{n+1} = 1
\end{aligned} \tag{43a}$$

Corrector step:

$$\begin{aligned}
&[\Phi^h_r M^{-1}\Phi^{hT}_r + \Phi^h_\pi J^{-1}\Phi^{hT}_\pi]\lambda = \frac{2\Phi^p}{\Delta t^2} + \frac{2\Phi^h_r}{\Delta t}(\dot r_n - \dot r^p_{n+1}) + \frac{2\Phi^h_\pi}{\Delta t}(\omega_n - \omega^p_{n+1}) + \Phi^h_r M^{-1} F + \Phi^h_\pi J^{-1}(T - \tilde\omega^h J\omega^h)\\
&\dot r_{n+1} = \dot r_n - \Delta t M^{-1}\Phi^{hT}_r \lambda + \Delta t M^{-1} F\\
&r_{n+1} = r_n + \frac{\Delta t}{2}(\dot r_{n+1} + \dot r_n)\\
&\omega_{n+1} = \omega_n - \Delta t J^{-1}\Phi^{hT}_\pi \lambda + \Delta t J^{-1} T - \Delta t J^{-1}\tilde\omega^h J\omega^h\\
&e_{n+1} = e_n + \frac{\Delta t}{2} G\left(\frac{1}{2}[\omega_{n+1} + \omega_n]\right)(e_{n+1} + e_n)\\
&e^T_{n+1}\, e_{n+1} = 1
\end{aligned} \tag{43b}$$

The scheme may also be summarized for the two-dimensional or generalized coordinate case without orientation parameters as follows:

Predictor step:

$$\begin{aligned}
&\left[\Phi_q M^{-1}\Phi^T_q\right]\lambda^p = \frac{\Phi}{\Delta t^2} + \frac{1}{\Delta t}\Phi_q \dot q_n + \Phi_q M^{-1} Q\\
&\dot q^p_{n+1} = \dot q_n + \Delta t M^{-1} Q - \Delta t M^{-1}\Phi^T_q \lambda^p\\
&q^p_{n+1} = q_n + \Delta t \dot q^p_{n+1}
\end{aligned} \tag{44a}$$

Corrector step:

$$\begin{aligned}
&\left[\Phi^h_q M^{-1}\Phi^{hT}_q\right]\lambda = \frac{2\Phi^p}{\Delta t^2} + \frac{2\Phi^h_q}{\Delta t}\left(\dot q_n - \dot q^p_{n+1}\right) + \Phi^h_q M^{-1} Q\\
&\dot q_{n+1} = \dot q_n - \Delta t M^{-1}\Phi^{hT}_q \lambda + \Delta t M^{-1} Q\\
&q_{n+1} = q_n + \frac{\Delta t}{2}(\dot q_{n+1} + \dot q_n)
\end{aligned} \tag{44b}$$

Note that this scheme requires solution of two symmetric positive-definite linear systems per time step.

IV. Baumgarte Stabilization

We briefly discuss our implementation of Baumgarte's stabilization method to make clear the basis for our comparisons in the following section. Baumgarte's stabilization technique may be used for this system in the following way. First, the second derivative of the constraint is stabilized by adding two terms with parameters α and β as follows:

$$\ddot\Phi + 2\alpha\dot\Phi + \beta^2\Phi = 0 \tag{45}$$

Note that without the stabilizing terms, the constraint would drift from zero. Making use of Eq. (4), this may be written as

$$\Phi_r \ddot r + \Phi_\pi \dot\omega + (\Phi_r \dot r)_r \dot r + (\Phi_\pi \omega)_\pi \omega + 2\alpha(\Phi_r \dot r + \Phi_\pi \omega) + \beta^2\Phi = 0 \tag{46}$$

Use of Eqs. (2) and (3) to eliminate $\ddot r$ and $\dot\omega$, we arrive at the linear system to be solved for the Lagrange multipliers:

$$\left\{\Phi_r M^{-1}\Phi^T_r + \Phi_\pi J^{-1}\Phi^T_\pi\right\}\lambda = \beta^2\Phi + 2\alpha(\Phi_r \dot r + \Phi_\pi \omega) + \Phi_r M^{-1} F + \Phi_\pi J^{-1}(T - \tilde\omega J\omega) + (\Phi_r \dot r)_r \dot r + (\Phi_\pi \omega)_\pi \omega \tag{47}$$

A first-order scheme using Baumgarte stabilization may easily be implemented by solving Eq. (47) for the Lagrange multipliers and then using Eqs. (14–17) and (22) to update the other variables. The first-order predictor and this variant of a first-order Baumgarte stabilization scheme were compared in [12]. Examination of

Eqs. (21) and (47) indicates that the parameter selections $\alpha = 0.5\Delta t^{-1}$ and $\beta = \Delta t^{-1}$ would result in our first-order predictor method and Baumgarte's stabilization method differing by only the last two terms in Eq. (47). Note that this parameter selection corresponds to a classical second-order system, with damping ratio equal to 0.5 and time constant proportional to Δt. We also note that if the final two terms in Eq. (47) are negligible, the schemes are identical and this parameter selection forces the constraint error to be zero (to within the order of the scheme) at the end of the time step [this can be seen from Eq. (20)]. In a linearized stability analysis [12], we found that the parameter selections $\alpha = \Delta t^{-1}$ and $\beta = \Delta t^{-1}$ that correspond to a damping coefficient of 1.0 and half the time constant as the previous parameter selection led to instability for the first-order method using Baumgarte stabilization. Using the parameter selections $\alpha = \Delta t^{-1}$ and $\beta = \Delta t^{-1}$ with a second-order method using Baumgarte stabilization (described next) results in a stable scheme. Therein lies the difficulty encountered in parameter selection for Baumgarte's stabilization. It is clear that the parameters should be proportional to Δt^{-1}, but the parameter selection is influenced by the stability characteristics and the order of the method, as well as by the dynamics of the system under consideration.

An attractive feature of the Baumgarte stabilization method is the ease with which a higher-order ODE solver may be used. To implement a typical higher-order solver, one must put the equations of motion into a state-space form:

$$\begin{bmatrix} \dot{r} & \ddot{r} & \dot{\omega} & \dot{e} \end{bmatrix}^T = f(r, \omega, e, t) \tag{48}$$

This is accomplished with Baumgarte stabilization as follows. First, every invocation of the function f on the right-hand side of the state-space form [Eq. (48)] must first solve Eq. (47) for the Lagrange multipliers. Then Eqs. (2), (3), and (10) are used to form the state-space form of the equations of motion:

$$\ddot{r} = M^{-1}\left(F - \Phi_r^T \lambda\right) \tag{49}$$

$$\dot{\omega} = J^{-1}\left(T - \tilde{\omega} J \omega - \Phi_\pi^T \lambda\right) \tag{50}$$

$$\dot{e} = G(\omega) e \tag{51}$$

Using this approach, it is very easy to apply any of the standard explicit higher-order ODE solvers to the dynamic system of equations. We shall use this approach to compare a second-order Runge-Kutta solution using Baumgarte stabilization and the second-order algebraic constraint scheme developed in the previous section.

V. Stability and Global Error Results

In what follows, we isolate the basic scheme and analyze the stability of the algorithm given by Eq. (44). We consider a homogeneous linearized system with constraints given by

$$\Phi(q) = Bq \tag{52}$$

where B is a constant coefficient matrix and the constraint gradient is thus

$$\Phi_q(q) = B \tag{53}$$

The Lagrange multiplier for the predictor step must satisfy the equation

$$A\lambda^p = \frac{1}{\Delta t^2} Bq(t) + \frac{1}{\Delta t} B\dot{q}(t) \tag{54}$$

where $A = BM^{-1}B^T$ and the predicted q^p and $\dot{q}^p$ are given by

$$\dot{q}^p = \dot{q}(t) - \Delta t M^{-1} B^T \lambda^p \tag{55}$$

$$q^p = q(t) + \Delta t \dot{q}(t + \Delta t) \tag{56}$$

The Lagrange multiplier for the corrector step must satisfy the equation

$$A\lambda = \frac{2}{\Delta t^2} Bq^p + \frac{2}{\Delta t} B[\dot{q}(t) - \dot{q}^p] \tag{57}$$

and the corrected q and $\dot{q}$ are given by

$$\dot{q}(t + \Delta t) = \dot{q}(t) - \Delta t M^{-1} B^T \lambda \tag{58}$$

$$q(t + \Delta t) = q(t) + \frac{\Delta t}{2}[\dot{q}(t + \Delta t) + \dot{q}(t)] \tag{59}$$

The Lagrange multipliers and predicted variables may now be eliminated and the resulting linearized discrete equations of motion are

$$\begin{bmatrix} q(t + \Delta t) \\ \dot{q}(t + \Delta t) \end{bmatrix} = X \begin{bmatrix} q(t) \\ \dot{q}(t) \end{bmatrix} \tag{60}$$

where

$$X = \begin{bmatrix} I - M^{-1}B^T A^{-1} B & \Delta t (I - M^{-1} B^T A^{-1} B) \\ \frac{-2}{\Delta t} M^{-1} B^T A^{-1} B & I - 2M^{-1} B^T A^{-1} B \end{bmatrix} \tag{61}$$

The condition for stability of this system of equations is

$$\rho(X) \leq 1 \tag{62}$$

where $\rho(X)$ is the spectral radius of the matrix X. A similar result may be derived for the Baumgarte method, with the result

$$\begin{bmatrix} q(t + \Delta t) \\ \dot{q}(t + \Delta t) \end{bmatrix} = \Lambda \begin{bmatrix} q(t) \\ \dot{q}(t) \end{bmatrix} \tag{63}$$

where

$$\Lambda = \begin{bmatrix} \mathrm{I} + \frac{\Delta t}{2}\Gamma(-\beta^2 \Delta t \mathrm{I} + \alpha\beta^2 \Delta t^2 \Gamma) & \Delta t \mathrm{I} - \frac{\Delta t}{2}\left(\frac{\beta^2 \Delta t^2}{2} + 2\alpha\Delta t\right)\Gamma + \alpha^2 \Delta t^3 \Gamma^2 \\ \Gamma(-\beta^2 \Delta t \mathrm{I} + \alpha\beta^2 \Delta t^2 \Gamma) & \mathrm{I} - \left(\frac{\beta^2 \Delta t^2}{2} + 2\alpha\Delta t\right)\Gamma + 2\alpha^2 \Delta t^2 \Gamma^2 \end{bmatrix} \tag{64}$$

and $\Gamma = M^{-1}B^T A^{-1} B$. The condition for stability for the Baumgarte method is

$$\rho(\Lambda) \leq 1 \tag{65}$$

To investigate the stability of the methods further, we consider the

simple problem of a planar double pendulum with links of equal length and mass. The equations of motion are written using generalized coordinates representing the Cartesian coordinates of the centers of mass and the rotation about the out-of-plane axis:

$$q = \begin{bmatrix} x_1 & y_1 & \theta_1 & x_2 & y_2 & \theta_2 \end{bmatrix}^T \tag{66}$$

The configuration is described by the four constraints:

$$\Phi = \begin{bmatrix} x_1 - \frac{L}{2}\sin(\theta_1) \\ y_1 - \frac{L}{2}\cos(\theta_1) \\ x_2 - x_1 - \frac{L}{2}\sin(\theta_1) - \frac{L}{2}\sin(\theta_2) \\ y_2 - y_1 - \frac{L}{2}\cos(\theta_1) - \frac{L}{2}\cos(\theta_2) \end{bmatrix} \tag{67}$$

The system is linearized about the vertical stable equilibrium position and the linearized constraint equation written using perturbation variables is

$$\Phi = \begin{bmatrix} x_1 - \frac{L}{2}\theta_1 \\ y_1 \\ x_2 - x_1 - \frac{L}{2}\theta_1 - \frac{L}{2}\theta_2 \\ y_2 - y_1 \end{bmatrix} \tag{68}$$

The linearized constraint Jacobian for this system is

$$B = \begin{bmatrix} 1 & 0 & -\frac{L}{2} & 0 & 0 & 0 \\ 0 & 1 & 0 & 0 & 0 & 0 \\ -1 & 0 & -\frac{L}{2} & -1 & 0 & -\frac{L}{2} \\ 0 & 1 & 0 & 0 & -1 & 0 \end{bmatrix} \tag{69}$$

We consider lengths of five units and mass of one unit and find that $\rho(X) \leq 1$ for all Δt, thus the algebraic constraint enforcement method is unconditionally stable. The stability behavior of Baumgarte's stabilization depends on the selection of the parameters α and β. For example, if we select parameters $\alpha = \Delta t^{-1}$ and $\beta = \Delta t^{-1}$, which give us a critically damped response with time constant proportional to Δt, we will find that the system has the stability limit $\Delta t \leq 0.0664$ s. This example highlights the difficulty in parameter selection for Baumgarte's stabilization technique. Improper choices for the parameters α and β often result in time-step limitations due to stability or in the time constants associated with constraint satisfaction being too slow. One of the advantages of the simple algebraic constraint enforcement scheme described in this paper is that the search for a good choice of parameters need not be undertaken. The stability analysis presented here is for the scheme given by Eq. (44) and does not include the integration of the orientation variables as given by Eq. (43), thus no stability result is provided for three-dimensional problems.

We next simulate the planar double pendulum for a time period of 10.0 s to present global convergence results. Both pendulum links are initially motionless and are oriented horizontally, with gravity in the vertical direction. Three simulations are run using time steps such that the higher-order truncation errors are negligible, and we may write expressions relating the approximate values, the exact values, and the global error as follows (written here for the constraint function):

$$\Phi = \Phi_{\text{exact}} + C\Delta t^n \tag{70}$$

where Φ is the approximate value, Φ_{exact} is the exact value, C is the coefficient of the global error term, and n is the order of the global error. Given three solutions at three time steps, Eq. (70) may be solved for Φ_{exact}, C, and n and the results are given in Table 1.

These results clearly indicate that for this case, the generalized coordinates and the constraints converge to second order globally, and the Lagrange multipliers are converging globally to slightly better than first order.

VI. Numerical Results

We present results from relatively simple examples to compare the two second-order integration methods differing in their treatment of constraints. For each method, the time step required to obtain a converged result for the coordinates is the same as each method in second order.

We begin by considering the slider-crank system considered in [2,5]. The system is defined by the generalized coordinates

$$q = \begin{bmatrix} \theta & \phi & x & y \end{bmatrix}^T \tag{71}$$

the force vector

$$Q = \begin{bmatrix} 0 & 0 & 0 & -mg \end{bmatrix}^T \tag{72}$$

the mass matrix

$$M = \begin{Bmatrix} J_1 & 0 & 0 & 0 \\ 0 & J_2 & 0 & 0 \\ 0 & 0 & m & 0 \\ 0 & 0 & 0 & m \end{Bmatrix} \tag{73}$$

and the constraint vector

Table 1 Global error results for planar double pendulum obtained using algebraic constraint enforcement

	$\Delta t = 0.005$ s	$\Delta t = 0.0025$ s	$\Delta t = 0.00125$ s	Exact [from Eq. (70)]	n
x_1	2.443655269310963e0	2.442965464018156e0	2.442790656734799e0	2.442713213864 02e0	1.98
y_1	−5.277783191794895e − 1	−5.309612759800720e − 1	−5.317648207729833e − 1	−5.320361837114458e − 1	1.99
θ_1	1.783508081764363e0	1.784810820126253e0	1.785139755818101e0	1.785250865278673e0	1.99
x_2	6.711359930283763e0	6.713351016578483e0	6.713852953944924e0	6.714022138581226e0	1.99
y_2	−2.765194090434459e0	−2.767952427377098e0	−2.768646375692474e0	−2.768879647789623e0	1.99
θ_2	2.323828290259711e0	2.321853408917590e0	2.321353974979965e0	2.321184918287540e0	1.98
$\dot{x}_1$	−1.819273871586672e − 1	−1.842799921770659e − 1	−1.848738194541881e − 1	−1.850743171218459e − 1	1.99
$\dot{y}_1$	−8.425945695282319e − 1	−8.479370879904064e − 1	−8.492773869483450e − 1	−8.497262382156855e − 1	1.99
$\dot{\theta}_1$	3.448043406049740e − 1	3.470922208260153e − 1	3.476665951459748e − 1	3.478591278120256e − 1	1.99
$\dot{x}_2$	8.358047330329132e0	8.340866444559893e0	8.336508225248394e0	8.335026936186582e0	1.98
$\dot{y}_2$	7.618758619232083e0	7.632854935537393e0	7.636424552087447e0	7.637635013353624e0	1.98
$\dot{\theta}_2$	−5.100854444583235e0	−5.104896782794190e0	−5.105912134225290e0	−5.106252716660437e0	1.99
λ_1	5.764615652238092e + 1	5.868436253318767e + 1	5.913991225254942e + 1	5.949608372080202e + 1	1.19
λ_2	−3.734488926265648e0	−4.052234009115540e0	−4.179614438038763e0	−4.264849660744103e0	1.32
λ_3	4.271195102102794e + 1	4.369108931718181e + 1	4.412375487226354e + 1	4.446631447036336e + 1	1.18
λ_4	−2.543944405550502e1	−2.574329960311427e1	−2.586977170351205e1	−2.595994467303359e + 1	1.26
Φ_1	2.012649042981707e − 7	2.638058038684221e − 8	3.369676981890279e − 9	−1.167900624849836e − 10	2.93
Φ_2	−4.337343506577440e − 8	−5.727478158412680e − 9	−7.331477647198881e − 10	3.077546804530299e − 11	2.91
Φ_3	2.580200099577823e − 6	3.347781205587097e − 7	4.257266783547209e − 8	−1.141905255467523e − 9	2.94
Φ_4	−2.301799984172348e − 6	−2.954876792138350e − 7	−3.741255971689839e − 8	6.845405262664950e − 10	2.96

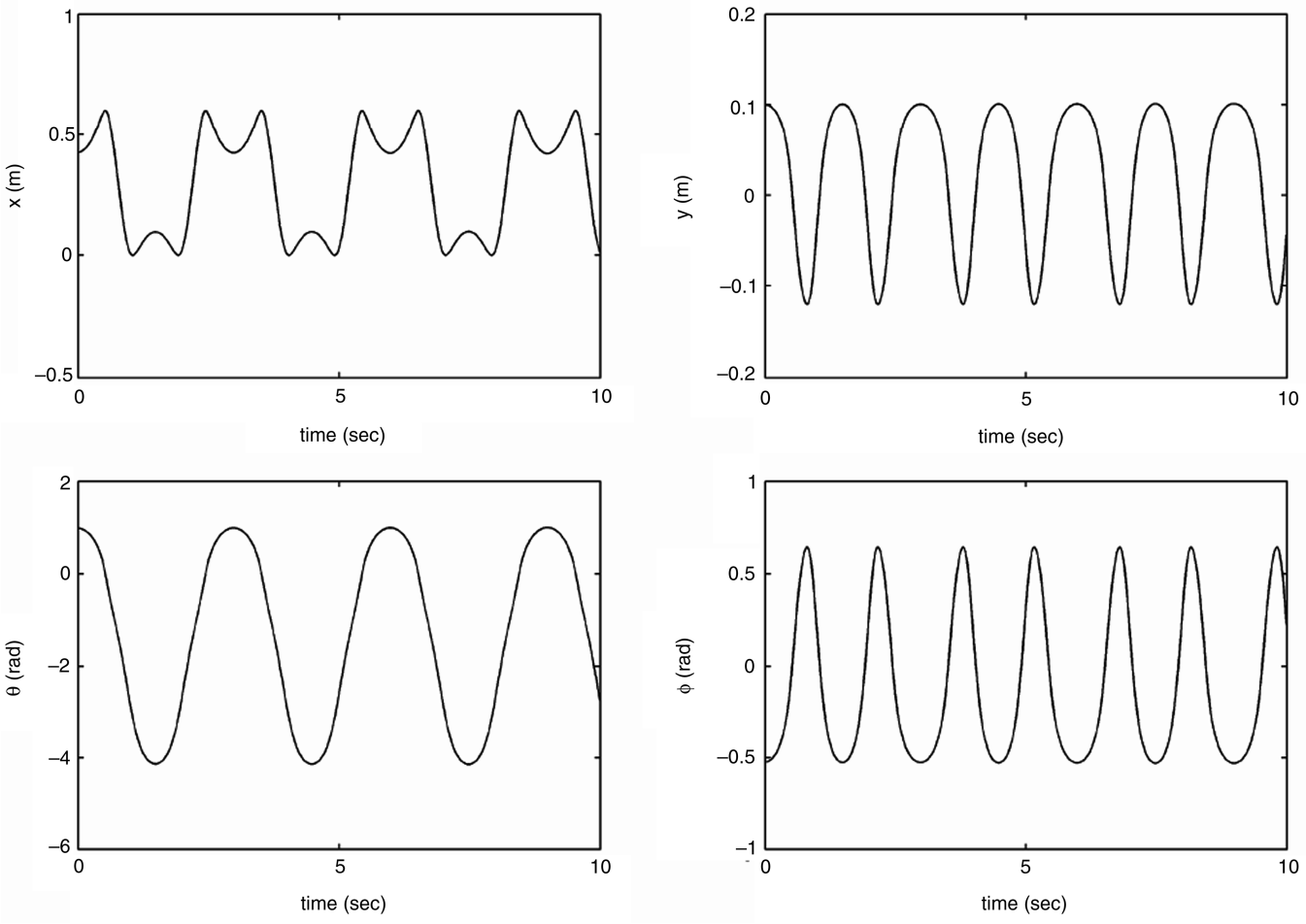

Fig. 1 Converged simulated generalized coordinates for the slider-crank example.

$$\Phi = \begin{Bmatrix} r\cos(\theta) + L_1\cos(\phi) - x \\ r\sin(\theta) + L_1\sin(\phi) - y \\ (L - L_1)\sin(\phi) + y \end{Bmatrix} \tag{74}$$

The parameters used are $L = 0.5$ m, $L_1 = 0.3$, $r = 0.3$, $g = 10.0\ \text{ms}^{-2}$, $m = 1$ kg, $J_1 = 0.045\ \text{kg}\cdot\text{m}^2$, and $J_2 = 33/4800\ \text{kg}\cdot\text{m}^2$, and the initial conditions are the same as in [2].

$$q(0) = \begin{bmatrix} 0.9851 & -0.5236 & 0.4256 & 0.1000 \end{bmatrix}^T \tag{75}$$

$$\dot{q}(0) = \begin{bmatrix} 0 & 0 & 0 & 0 \end{bmatrix}^T \tag{76}$$

We use this system to study accuracy and convergence properties for the methods discussed earlier. We note that because this system has no nonlinear terms resulting from three-dimensional orientation dynamics, our second-order method has no time-step stability limit. Figure 1 shows the converged (to within plotting accuracy) solutions for the generalized coordinates over a time duration of 10 s. The time step used to obtain this converged solution (for both methods) is $\Delta t = 0.01$ s. The Baumgarte stabilized simulations in this example use the parameter selections $\alpha = \Delta t^{-1}$ and $\beta = \Delta t^{-1}$, which were found to be optimal based upon numerical experimentation.

Figure 2 shows the time variation of the magnitude of the constraint vector for this simulation. We observe that the magnitude of the constraint errors is comparable with the magnitude of the constraint error for our method, being smaller on average by a factor of 3.78 (this is shown in Table 1).

To verify the convergence properties of the methods, we consider the magnitude of the constraint error averaged over the duration of the simulation. We consider two simulations with time steps $\Delta t =$ 0.02 s and $\Delta t = 0.01$ s and we note that the second time step corresponds to the converged result shown in Fig. 1. To verify convergence properties, we express this average magnitude of the constraint error using the truncation error and the exact value (theoretically equal to zero):

$$\bar{\Phi} = \bar{\Phi}_{\text{exact}} + C\Delta t^n = C\Delta t^n \tag{77}$$

where $\bar{\Phi}$ is the magnitude of the constraint averaged over the duration of the simulation, $\bar{\Phi}_{\text{exact}}$ is the exact value (set to zero), and C is an unknown coefficient. Equation (77) is applied to the two sets of simulation results and the exponent n, representing the local

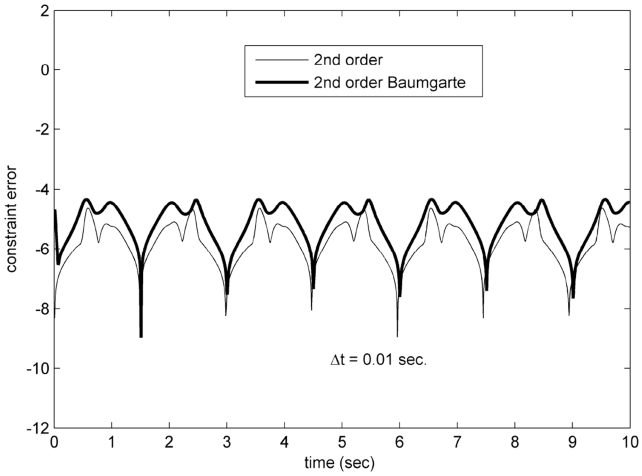

Fig. 2 Slider-crank example of $\log_{10}$ of $|\Phi|$.

Table 2 Convergence verification results for the slider-crank example

	$\Delta t = 0.02$ s	$\Delta t = 0.01$ s	n
$\bar{\Phi}$ Baumgarte second order	1.0856e − 4	1.4877e − 5	2.87
$\bar{\Phi}$ second order	3.1960e − 5	3.9802e − 6	3.01
$\bar{\Phi}$ first order	1.0038e − 3	2.5339e − 4	1.99

truncation error, is obtained. Table 2 gives these results and the result for the same calculation applied to the first-order scheme developed earlier.

The results indicate that as expected, Baumgarte's method integrated with a second-order method and our method both converge to third order locally and our first-order method converges to second order locally. Our second-order method is more accurate in terms of the magnitude of the constraint error, but the solutions obtained by both methods may be characterized as being comparable and accurate to second order. This system is conservative and another comparison may be made by inspecting the change in total energy (theoretically zero). We define the relative change in total energy as

$$\varepsilon_E = \frac{|E_o - E|}{E_0} \tag{78}$$

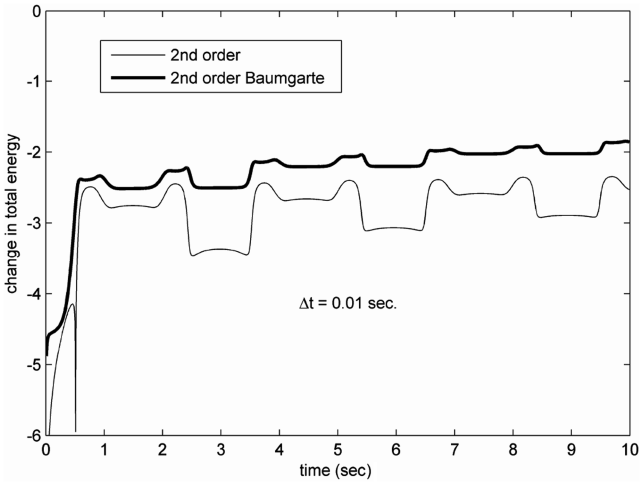

Fig. 3 Slider-crank example of $\log_{10}$ of ε_E.

Figure 3 gives this quantity and we observe that for this case, our method is preserving energy more accurately, but just as with the magnitude of the constraint error, the results are comparable.

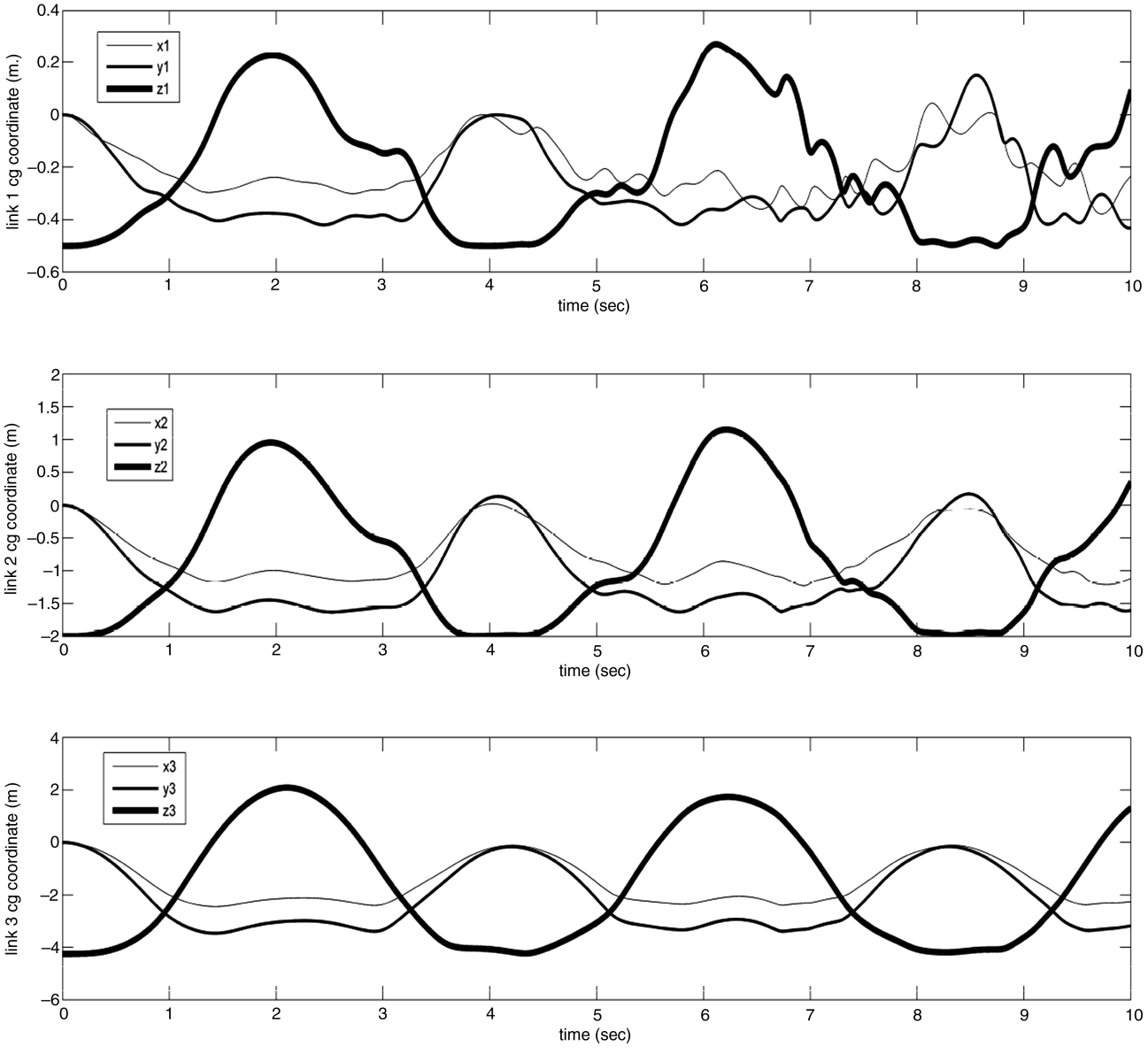

Fig. 4 Converged simulated center of gravity coordinates for the pendulum example.

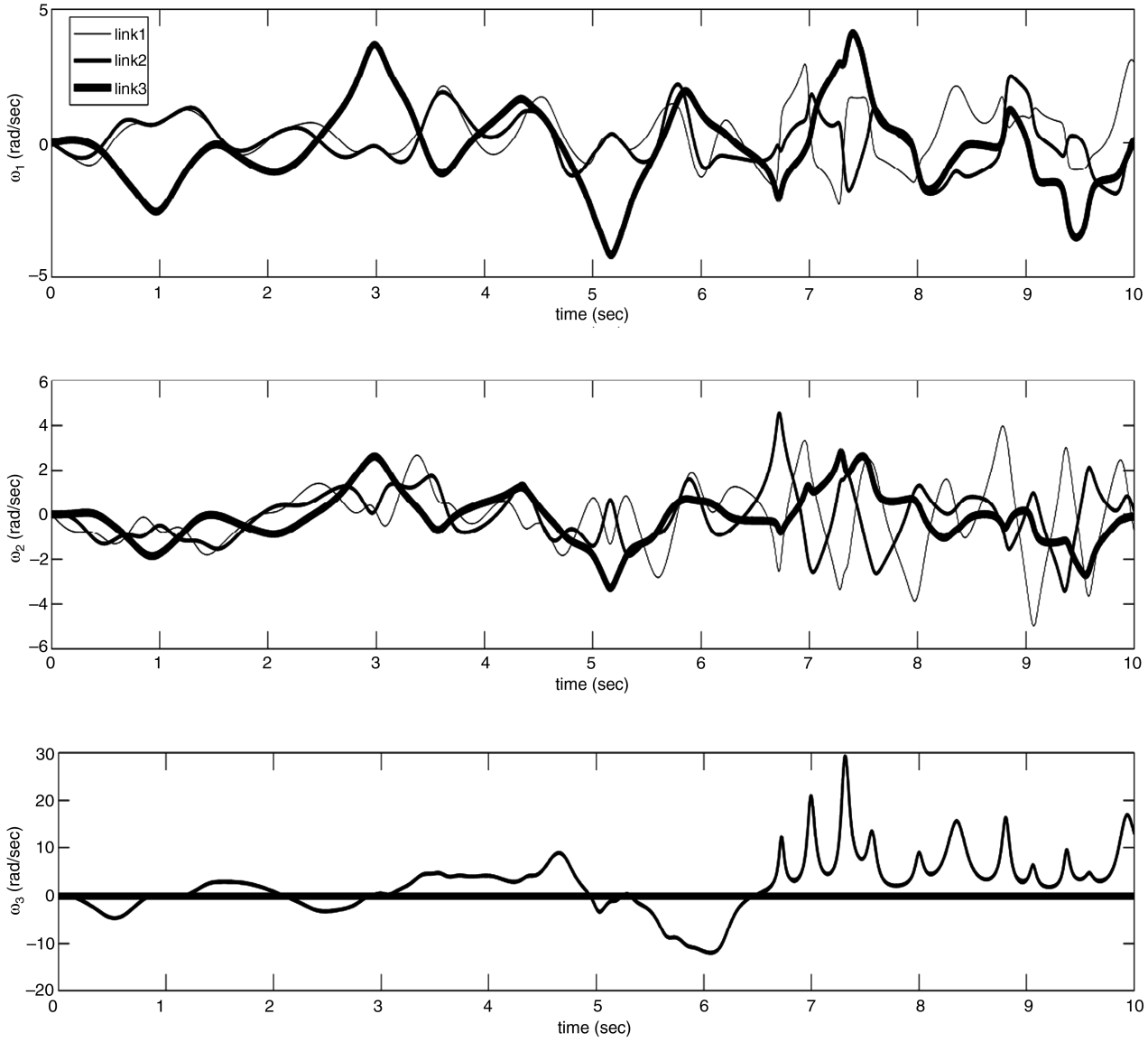

Fig. 5 Converged simulated angular velocities for the pendulum example.

We next consider a three-dimensional, three-link pendulum, with each link having a square cross section of dimension that is one-tenth the link length. The three link lengths are 1.0, 2.0, and 2.5 m. The short link is fixed to ground with a spherical joint, the second link is fixed to the first link with a spherical joint, and the third link is fixed to the second link with a pin joint where the axis of the pin is perpendicular to links two and three. The resulting constraint vector has dimension 11, and the constraint functions and associated Jacobians are tabulated by Haug [13] and are easily programmed. The links are originally oriented vertically (downward in the z direction) with zero initial velocities, and the gravitational vector is given by

$$g = -10\begin{bmatrix} 1/2 & \sqrt{2}/2 & 1/2 \end{bmatrix}^T \text{ m/s}^2 \tag{79}$$

Optimal Baumgarte parameters for this example were found to be $\alpha = 0.5\Delta t^{-1}$ and $\beta = \Delta t^{-1}$, and we simulate this system for a time duration of 10.0 s. Converged (to within plotting accuracy) results for the center of gravity coordinates and the angular velocities are found for both methods at a time step of $\Delta t = 2.5 \times 10^{-5}$ s. Figure 4 shows the converged center of gravity coordinate, and Fig. 5 gives the angular velocities of each link expressed in body-fixed frames. Note that the third component of the angular velocities of links 2 and 3 should be identical, due to the pin joint, and this is reflected in Fig. 5.

Figure 6 gives the time variation of the magnitude of the constraint vector. For this simulation, the average Baumgarte method constraint error is approximately four orders of magnitude larger than the average constraint error for our method.

As in the previous example, we investigate the convergence of the constraint error by applying Eq. (77) to simulation results obtained using time steps $\Delta t = 5.0 \times 10^{-5}$ and $\Delta t = 2.5 \times 10^{-5}$ s.

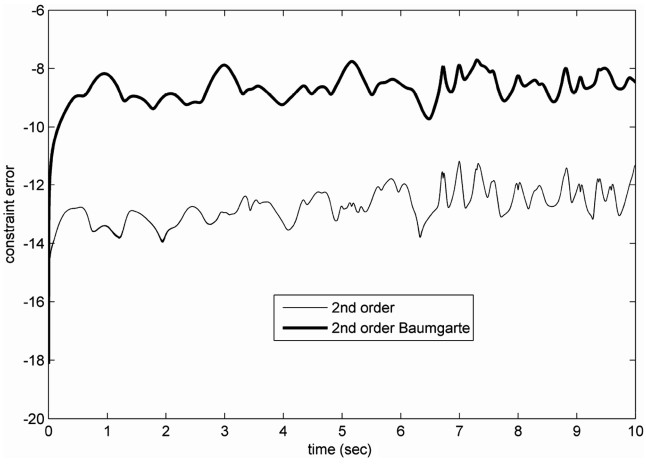

Fig. 6 Pendulum example of $\log_{10}$ of $|\Phi|$.

Table 3 Convergence verification results for the pendulum example

	$\Delta t = 5.0 \times 10^{-5}$ s	$\Delta t = 2.5 \times 10^{-5}$ s	n
$\bar{\Phi}$ Baumgarte second order	1.3712e − 8	3.4275e − 9	2.00
$\bar{\Phi}$ second order	3.4046e − 12	4.3761e − 13	2.96

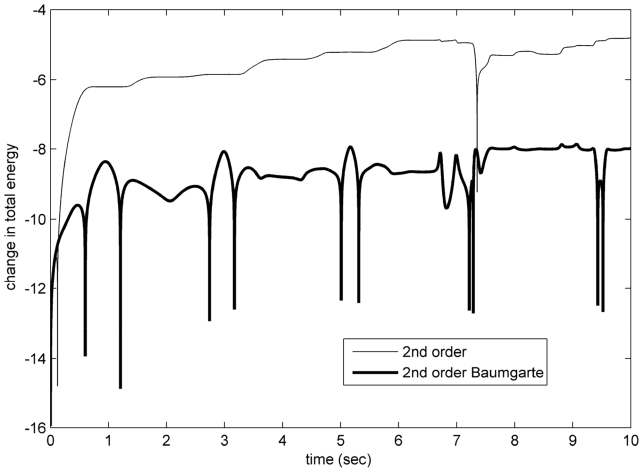

Fig. 7 Pendulum example of $\log_{10}$ of ε_E.

The results are given in Table 3 and show that our second-order method retained second-order accuracy, whereas the version of the Baumgarte stabilization method used is converging only to first order. This is likely due to the artificial time constants that the Baumgarte stabilization method adds to the system dynamics. If we were using an implicit method with Baumgarte stabilization, the parameters α and β parameters could be increased in size, thus decreasing the associated time constants, but the explicit method used here is stability-limited and the parameters used are near the stability limit. The interplay between the artificial time constants, stability, and constraint satisfaction is a complication that must be faced when using Baumgarte stabilization.

Figure 7 shows the relative change in total energy [defined by Eq. (78)] calculated using simulation results for the two methods. As shown in the figure, the Baumgarte stabilized results are approximately four orders of magnitude better than the results for our method.

Given these mixed results, it is appropriate to say that the methods are comparable in terms of overall accuracy. The center of gravity coordinates and the angular velocities converge at the same time step, and the Baumgarte method used in this work provided less accurate constraint satisfaction but more accurate energy conservation. For the results shown, the errors in constraint satisfaction and energy conservation for both methods are small enough that they do not manifest themselves through perceptible differences in the solutions for center of gravity coordinates and angular velocities.

VII. Conclusions

A second-order integration scheme including algebraic constraint satisfaction was developed and compared with a second-order formulation using Baumgarte stabilization. The philosophy of the method is to expand the constraint at the new time in a Taylor series to the same order as the integration method used. In the simulations presented, as well as in our experience with the methods, the results are comparable. Generally, we get more accurate results in terms of constraint satisfaction, but the overall results are comparable when optimal values for the Baumgarte stabilization parameters are found. Our method is parameter-free and the linear systems that must be solved are symmetric and positive definite. Baumgarte stabilization requires the user to determine two parameters. In addition, the linear systems that must be solved are identical to the linear systems that must be solved with our method, thus both methods require the same computational cost. In summary, our method is parameter-free and second order, whereas Baumgarte stabilization is flexible and easily implemented with higher-order solvers.

Acknowledgments

This work was supported by the Korean Research Foundation, funded by the Korean Government, Ministry of Education and Human Resource Development, Basic Research Promotion Fund, grant KRF-2006-003-D00499.

References

[1] Baumgarte, J., "Stabilization Of Constraints and Integrals of Motion in Dynamical Systems," *Computer Methods in Applied Mechanics and Engineering*, Vol. 1, No. 1, 1972, pp. 1–16.

[2] Wu, S. D., Chiou, J. C., and Lin, Y. C., "Modified Adams-Moulton Predictor-Corrector Method in Solving Multibody Dynamical Systems," *Mechanics of Structures and Machines*, Vol. 28, No. 2, 2000, pp. 201–218.

[3] Lin, S.-T., and Huang, J.-H., "Parameters Selection for Baumgarte's Constraint Stabilization Method Using the Predictor-Corrector Approach," *Journal of Guidance, Control, and Dynamics*, Vol. 23, No. 3, 2000, pp. 566–570.

[4] Lin, S.-T., and Huang, J.-H., "Stabilization of Baumgarte's Method Using the Runge-Kutta Approach," *Journal of Mechanical Design*, Vol. 124, No. 4, 2002, pp. 633–641.

[5] Park, K. C., and Chiou, J. C., "Stabilization of Computational Procedures for Constrained Dynamical Systems," *Journal of Guidance, Control, and Dynamics*, Vol. 11, No. 4, 1988, pp. 365–370.

[6] Ascher, U. M., Chin, H., Petzold, L. R., and Reich, S., "Stabilization of Constrained Mechanical Systems with DAEs and Invariant Manifolds," *Mechanics of Structures and Machines*, Vol. 23, No. 2, 1995, pp. 125–157.

[7] Negrut, D., Haug, E. J., and German, H. C., "An Implicit Runge-Kutta Method for Integration of Differential Algebraic Equations of Multibody Dynamics," *Multibody System Dynamics*, Vol. 9, No. 2, 2003, pp. 121–142.

[8] Aghili, F., and Piedboeuf, J.-C., "Simulation of Constrained Multibody Systems Based on Projection Operator," *Multibody System Dynamics*, Vol. 10, No. 1, 2003, pp. 3–16.

[9] Brenan, K. E., Campbell, S. L., and Petzold, L. R., *Numerical Solution of Initial-Value Problems in Differential-Algebraic Equations*, Society for Industrial and Applied Mathematics (SIAM), Philadelphia, 1996, pp. 41–74.

[10] Hong, M., Choi, M., Jung, S., Welch, S., and Trapp, J., "Effective Constrained Dynamic Simulation Using Implicit Constraint Enforcement," *2005 IEEE International Conference on Robotics and Automation*, Inst. of Electrical and Electronics Engineers, Piscataway, NJ, 2005, pp. 4531–4536.

[11] Hong, M., Welch, S., and Choi, M., *Intuitive Control of Dynamic Simulation using Improved Implicit Constraint Enforcement*, Lecture Notes in Computer Science, Vol. 3398, Springer–Verlag, New York, 2005, pp. 315–323.

[12] Hong, M., Welch, S., Trapp, J., and Choi, M., *Implicit Constraint Enforcement for Rigid Body Dynamic Simulation*, Lecture Notes in Computer Science, Vol. 3991, Springer–Verlag, New York, 2006, pp. 490–497.

[13] Haug, E. J., *Computer Aided Kinematics and Dynamics of Mechanical Systems*, Prentice–Hall, Englewood Cliffs, NJ, 1989, pp. 345, 353, 357.

[14] Greenwood, D., *Advanced Dynamics*, Cambridge Univ. Press, New York, 2003, pp. 382–383.